J Mater Sci: Mater Med (2011) 22:1183–1193
DOI 10.1007/s10856-011-4295-6

Fabrication of novel PLA/CDHA bionanocomposite fibers for tissue engineering applications via electrospinning

Huan Zhou · Ahmed H. Touny · Sarit B. Bhaduri

Received: 26 January 2011 / Accepted: 14 March 2011 / Published online: 24 March 2011

Abstract The main theme here is to fabricate PLA (poly lactic-acid)/CDHA (carbonated calcium deficient hydroxyapatite) bionanocomposites, where both the constituents are biocompatible and biodegradable with one dimension in nanometer scale. Such materials are important in tissue engineering applications. The bionanocomposite fibers were fabricated via electrospinning. There are two important signatures of this paper. First, CDHA, rather than HA, is added to PLA as the second phase. As opposed to HA, CDHA mimics the bone mineral composition better and is biodegradable. Therefore, PLA/CDHA fibers should have better biodegradability while maintaining a physiological pH during degradation. To the best of our knowledge, this is the first attempt of electrospinning of such a composite. Second, the CDHA nanoparticles were synthesized using the benign low temperature biomimetic technique, the only route available for the retention of carbonate ions in the HA lattice. The structural properties, degradation behavior, bioactivity, cell adhesion, and growth capability of as-fabricated PLA/CDHA bionanocomposites were investigated. The results show that the incorporation of CDHA decreased PLA fiber diameters, accelerated PLA degradation, buffered pH decrease caused by PLA degradation, improved the bioactivity and biocompatibility of the scaffold. These results prove that PLA/CDHA bionanocomposites have the potential in tissue regeneration applications.

H. Zhou (✉)
Department of Bioengineering, The University of Toledo, Toledo, OH, USA
e-mail: Huan.Zhou@Rockets.utoledo.edu

A. H. Touny
Department of Chemistry, Helwan University, Ain Helwan, Cairo, Egypt

S. B. Bhaduri
Department of Mechanical, Industrial and Manufacturing Engineering, The University of Toledo, Toledo, OH, USA

S. B. Bhaduri
Department of Surgery (Dentistry), The University of Toledo, Toledo, OH, USA

1 Introduction

The major theme of this work is to fabricate PLA (poly lactic acid)/CDHA (carbonated calcium deficient hydroxyapatite) bionanocomposites for tissue engineering applications. To the best of our knowledge, this is the first example of an electrospun PLA/CDHA bionanocomposite scaffold for tissue engineering. As explained in the following, the presence of CDHA is critical to proper functioning of PLA based scaffold, yet has not been attempted before. For such applications, electrospinning has emerged as a potential process for the fabrication of temporary fibrous scaffolds to serve as a substrate for implanted cells and newly formed tissues [1]. The term "bionanocomposites" can be defined by referring to the field of nanocomposites. The latter term has been coined by adding the prefix "Bio" to "nanocomposites". Roy and Roy originally used "nanocomposites" in describing the resulting structure of sol-gel processed ceramics and glasses [2, 3]. Komarneni presented a review of such developments [4]. By following the definition of nanocomposites, bionanocomposites can be defined by their constituents and their size. As opposed to single-phase materials, nanocomposites are heterogeneous materials consisting of two or more phases with the restriction that at least one dimension of the constituents should of the order of 1–50 nm range [4]. However, such size restrictions are

not rigorously applied as along as one of the constituents meets the criterion. The constituents can be organic or inorganic in any combination. A seminal paper laying out the concepts of bionanocomposites has been published by Dardar et al. [5]. In our specific case, an organic material (PLA) is the matrix and an inorganic material (CDHA) is the second phase. Both the matrix and the second phase are in nanometer scale.

The reason for the choice of PLA as the matrix is simple: it is a FDA approved biomaterial used for applications as sutures, pins, screws and drug delivery systems [6, 7]. It can also be used to fabricate fibrous scaffolds via electrospinning [1]. However, when it comes to tissue engineering, PLA has disadvantages such as low cell adhesion due to its hydrophobic surface property, and inflammatory reactions in vivo caused by its degradation product, lactic acid [8, 9]. The incorporation of Calcium Phosphate (CaP) particles into PLA matrix can buffer the localized pH decrease, and improve cell adhesion, osteoconductivity, and mechanical properties [10, 11].

There are two important signatures of this work. First is the use of CDHA as the second phase. Of CaP materials used in composite fabrication, hydroxyapatite (HA, $Ca_{10}(PO_4)_6(OH)_2$) is a very common second phase [12]. While HA is structurally similar to the main inorganic component of nature bone, it is still compositionally different. The mineral component of bone is carbonated calcium phosphate (CDHA) with small amounts of sodium (Na^+), potassium (K^+), magnesium (Mg^{2+}), carbonate (CO_3^{2-}) and water (H_2O) along with the major mineral content of calcium (Ca^{2+}) and phosphate (PO_4^{3-}) [13]. As a result of this subtle difference, CDHA is a bioactive material, while HA is not, in spite of its biocompatibility. Unfortunately, most of the papers reported in the literature use HA as the second phase in fabricating composites with a whole range of biopolymers as matrices including PLA [10, 12, 14].

Second, nanocrystalline CDHA powders are synthesized using a biomimetic process. Being a benign low temperature process, it can retain the carbonate ions in CDHA lattice. No high temperature technique can achieve this. Kokubo has developed simulated body fluid (SBF) to biomimetically synthesize CDHA coatings [15]. The process involves immersing metallic, ceramic, or polymeric substrates into SBF solution held at 37°C. Such a process must meet three criteria: (1) the SBF composition should closely mimic the ionic species and concentrations of human plasma; (2) the pH of the SBF should be fixed at that of the human blood (7.40); (3) continuous process temperature should always be kept at the physiologic temperature of 37°C. A composition of SBF (c-SBF), pioneered and popularized by Kokubo, meets the above criteria [15]. The problem associated with c-SBF is that concentration of HCO_3^- is 4.2 mM, which is much less than that of human plasma. Tas first realized this problem and revised this original c-SBF composition, which we refer to as (t-SBF) [16]. There are several other compositions also available in the literature [17–19]. Our group has provided ample proof of the efficiency of t-SBF in fabricating monolithic CDHA coatings [20, 21]. During the CDHA deposition process, an amorphous calcium phosphate precursor is always present [22, 23]. Such precursors are considered as transient solution precursors for the formation of CDHA precipitates with a size range of 0.7–1.0 nm. The CaP clusters in the solution form apatite nuclei either on the surface of a substrate or in the SBF solution. Those nucleated on the substrate can further grow into a CDHA coating layer, while those nucleated in the solution form CDHA precipitates [24]. In this work, these nucleated particles are collected for further use. In addition, during the nucleation and precipitation processes, trace elements can be combined into lattice structure. These CDHA precipitates have the potential to be ideal second phase materials for biopolymer matrix because they are biocompatible, as well as bioactive.

Formation of monolithic PLA/CDHA composites has been reported in the literature before. Durucan et al. [25] reported fabrication of CDHA-PLA/PLGA composites via the hydrolysis of TCP-PLA/PLGA composites. Zhang et al. [26] soaked PLA scaffold into simulated body fluid (SBF) to deposit CDHA coatings on PLA surface. Rakovsky et al. [27] fabricated CDHA/PLA nanocomposite via high pressure consolidation, CDHA was synthesized via wet chemical synthesis. But this is the first time that electrospun PLA/CDHA bionanocomposites have been fabricated. This paper describes: (1) the synthesis of CDHA using the t-SBF, (2) incorporate the CDHA nanoparticles into the nanofibers of PLA via the process of electrospinning, and (3) to evaluate the physical properties, degradation behavior, bioactivity, cell attachment, and growth capability of as-fabricated PLA/CDHA bionanocomposites.

2 Materials and methods

2.1 CDHA powders synthesis

CDHA was synthesized using modified 1.5 × t-SBF, with reduced content of Tris-Base compared to conventional 1.5 × t-SBF reported before [20]. The compositions are shown in Table 1. The reagents were dissolved in solution one by one, and added based on the order listed in Table 1. $NaHCO_3$ and Na_2SO_4 were purchased from Acros Organics. NaCl, KCl, NaH_2PO_4, $MgCl_2{\cdot}6H_2O$, $CaCl_2{\cdot}2H_2O$, Tris-base buffer ($C_4H_{11}NO_6$), and HCl were purchased from Fisher Scientific. The solution was later stored at 37°C environment for 24 h. Subsequently, CDHA

Table 1 Modified 1.5 × t-SBF solution composition for a total volume of 1 l

Order	Reagent	Amount (g)
1	NaCl	9.8184
2	$NaHCO_3$	3.4023
3	KCl	0.5591
4	Na_2HPO_4	0.2129
5	$MgCl_2{\cdot}6H_2O$	0.4574
6	1M HCL	15 ml
7	$CaCl_2{\cdot}2H_2O$	0.5822
8	Na_2SO_4	0.1080
9	Tris-Base	6.063
10	1 M HCl	29 ml

precipitates were collected after filtration and dried in oven overnight. Further characterization was applied to prove such precipitates were exactly CDHA.

2.2 PLA/CDHA solution preparation

PLA pellets were supplied by Jamplast (Ellisville, MO). The weight average molecular weight (Mw) and poly dispersity of PLA are 114,000 and 1.435, respectively. These values were determined by gel permeation chromatography relative to polystyrene standards using a Shimadzu LC–10ADVP liquid chromatography equipped with a Shimadzu ELSD-LT ultraviolet (UV) detector (Columbia, MD). Chloroform ($CHCl_3$) and Dimethylformamide (DMF) were used as medium for the presentation of electrospinable mixtures and were purchased from Fisher Scientific. PLA pellets were initially dissolved in chloroform. Following that, CDHA precipitates were added to PLA solution to make a mixture. To uniformly disperse CDHA crystals in PLA solution, mixture was treated by 1 h ultrasonication to destroy CDHA agglomerates. After further addition of DMF to the mixture and 4 h of stirring, the solution was ready for electrospinning. The volume ratio of chloroform and DMF was adjusted to tailor the fiber surface morphology (Table 2).

2.3 Electrospinning approach

A horizontal electrospinning setup was used in this study to fabricate fibrous composite scaffold. It was composed of a high voltage power supply, a pump, a syringe, a flat tip needle and a conducting collector plate. In general, the morphology of fibers can be influenced by various processing parameters such as applied voltage, feeding rate, and working distance [2]. The operating parameters applied in the experiment were based on our previous research (unpublished data). A certain volume of PLA/CDHA solution (constant total mass/volume ratio at 1:10 (g/ml)) was loaded into the syringe and injected through a needle (gauge 22) at constant operating parameters to fabricate PLA/CDHA fibers containing 25% CDHA mass ratio; neat PLA fibers were also electrospun with the same operating parameters as control (Table 2). Fibers were collected and left to dry in a fume hood to remove residual solvents. Once no weight loss of as-produced fibers was observed by using XP105 DeltaRange analysis balance (Mettler Toledo), residual solvents were considered to be totally removed.

2.4 Physical evaluation

CDHA nanocrystals, PLA pellets, and as-fabricated PLA/CDHA fibers all were characterized by X-ray diffraction (XRD, Ultima III, Rigaku) with monochromated Cu Kα radiation, operated at voltage 40 kV and 44 mA setting. All samples were examined at 2θ angles from 10 to 45° at a scanning speed of 1°/min. Fourier transform infrared spectroscopy (FTIR, UMA-600 Microscope, Varian Excalibur Series) was also applied for chemical analysis of nanocrystals and fibers. The transmittance of each sample was recorded with 256 scans with resolution of 4 cm^{-1} between 4000 and 700 cm^{-1}. The morphological features of precipitates and fibers were visualized by scanning electron microscope (SEM, S4800, Hitachi). Energy dispersive X-ray spectroscopy (EDX) analysis was applied to examine the distribution of precipitates in fibers. Nano-structures of precipitates and PLA/CDHA composites were investigated using transmission electron microscopy (TEM, HD-2300, Hitachi) with a voltage 200 kV and the zeta contrast mode.

2.5 In vitro degradation tests

To clearly prove the degradation efficiency of CDHA against HA, a comparison of degradation between CDHA and synthesized HA was carried out. HA was synthesized via chemical method using $Ca(OH)_2$ and H_3PO_4. Both the chemicals were purchased from Fisher Scientific. A measured weight of 0.05 g powders was added into tubes containing 15 ml phosphate buffer solution (PBS) (pH 7.4), and all tubes are incubated in vitro at 37°C for different times. Three samples of each type were taken out at the end of each degradation period, and pH change of the PBS with time was measured. Centrifugation was applied to pipette out PBS, and powders were washed using DI water and dried in air to remove residential water. The weights of dried powders were measured.

PLA/CDHA and PLA fibers (chloromform:DMF ratio is 7:3) were electrospun on to microscope cover glasses (18 mm diameter, purchased from Fisher Scientific) for in vitro degradation test. The weight of each glass substrate

Table 2 Mixture compositions and working conditions

No.	CDHA ratio (%)	Chloroform:DMF (ml/ml)	Working distance (cm)	Applied voltage (kV)	Feeding rate (ml/h)
1	0	9:1	25	20	1
2	0	7:3	25	20	1
3	25	9:1	25	20	1
4	25	7:3	25	20	1

and sample were recorded and placed in closed tubes containing 25 ml PBS and incubated in vitro at 37°C for different times. Three samples of each type were taken out from the incubator at the end of each degradation period, pH values of the PBS and the weights of the dried samples were measured.

2.6 Bioactivity test

For a material to be bioactive in vivo, it must have the ability to induce apatite formation on its surface in vitro. In order to show that the bioactivity of CDHA and PLA was maintained in the process of mixture preparation and electrospinning, PLA/CDHA and PLA fibers (chloromform:DMF ratio is 7:3) were electrospun to microscope cover glass (18 mm diameter, purchased from Fisher Scientific) for bioactivity test. Samples were placed in closed tubes containing 25 ml 1.5 × t-SBF and incubated in vitro at 37°C for 1 week with solution replenished every 48 h. The chemical compositions of 1.5 × t-SBF are shown in Table 3. The apatite formation on fibers surface were characterized using XRD and SEM.

2.7 Osteoblast cell culture

7F2 mouse osteoblast cells (CRL-12557, American Type Culture Collection) were used for cell culture studies on PLA/CDHA (3:1) fibers (chloromform:DMF ratio is 7:3). PLA/CDHA fibers were fixed onto microscope cover glass strips (Fisher Scientific) to ensure they can settle in the wells with medium. PLA fibers were also fixed as controls, and microscope cover glass strips were used as blank. Osteoblast cells are mononucleate cells that are responsible for bone formation. Cells were first grown at 37°C and 5% CO_2 in alpha minimum essential medium (α-MEM, Thermo Scientific HyClone), augmented by 10% Fetal Bovine Serum (FBS, Thermo Scientific HyClone). The culture medium was replenished every other day until the cell reached a confluence of 90%. Osteoblasts were seeded to wells (BD Flacon™ 12 wells cell culture plates) of sterilized PLA and PLA/CDHA fibers (chloromform:DMF ratio is 7:3), approximately 20,000 osteoblast cells were seeded to each well. Cell numbers on samples were counted after 24 h, 4 days and 7 days using CytoTox 96® Non-Radioactive Cytotoxicity Assay kit (Promega). For statistical analysis, all experiments were performed at least triplicate. Osteoblast morphology after attachment was examined using SEM. Glutaraldehyde and HMDS were purchased from Fisher Scientific, ethanol was purchased from Pharmco-Aaper. These chemicals were used for SEM samples preparation. Prior to SEM characterization, samples were soaked in primary fixative of 3.5% glutaraldehyde. Subsequently samples were washed by PBS buffer and dehydrated with increasing concentrations of ethanol (30, 50, 70, 90, 95 and 100%) for 15 min each. After the dehydration of ethanol, samples were kept in solution of HMDS (hexamethyldisilazane)-ethanol (1:2, v/v) for 15 min, HMDS-ethanol (2:1, v/v) for 15 min, and 2 changes for 15 min each with 100% HMDS. Finally, HMDS was removed and samples were air dried in a hood overnight. The samples were then ready to be sputter coated with gold for SEM characterization.

Table 3 1.5 × t-SBF solution omposition for a total volume of 1 l

Order	Reagent	Amount (g)
1	NaCl	9.8184
2	$NaHCO_3$	3.4023
3	KCl	0.5591
4	Na_2HPO_4	0.2129
5	$MgCl_2{\cdot}6H_2O$	0.4574
6	1 M HCL	15 ml
7	$CaCl_2{\cdot}2H_2O$	0.5822
8	Na_2SO_4	0.1080
9	Tris-Base	9.0855
10	1 M HCl	50 ml

3 Results

3.1 Physical evaluation

The XRD patterns of precipitated nanocrystals, PLA pellets, PLA fibers and PLA/CDHA fibers are shown in Fig. 1. For precipitates, the main XRD peaks at 2θ angle 25.9 and 31.8° confirmed the formation of HA lattice (JCPDS-ICDD card no. 18-03030). The crystal domain sizes of precipitates along the c direction were calculated by JADE software based on Scherrer's equation using (002) diffraction peak,

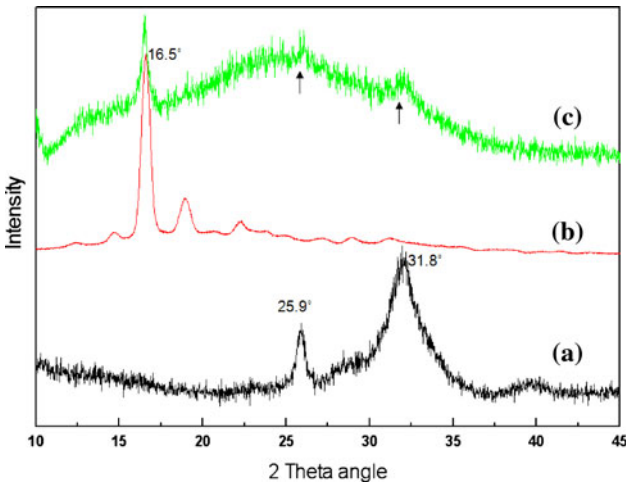

Fig. 1 XRD patterns of **a** CDHA nanocrystals, **b** PLA pellets, **c** PLA/CDHA fibers

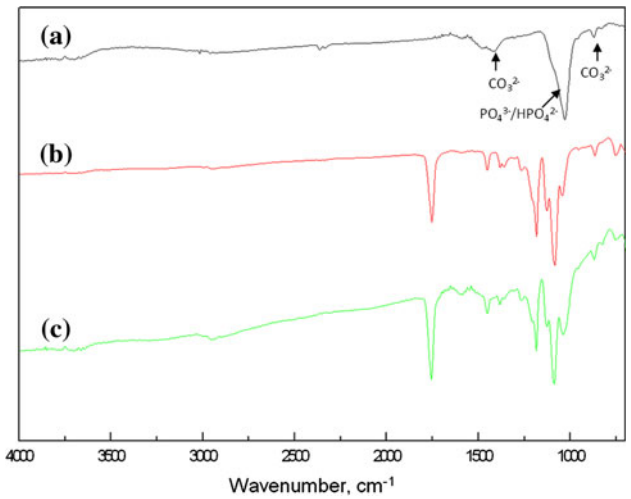

Fig. 2 FTIR data of **a** CDHA nanocrystals, **b** PLA pellets, **c** PLA/CDHA fibers

and were equal to 210 Å. PLA pellets examined by XRD showed high crystallite with a strong peak observed at 16.5°. Both PLA and CDHA XRD peaks were observed on the XRD patterns of PLA/CDHA fibers, which confirmed the presence of CDHA and PLA in the composite fibers.

The FTIR data of nanocrystalline CDHA, PLA, and PLA/CDHA fibers are shown in Fig. 2. From FTIR data of CDHA, the presence of carbonate in nanocrystalline CDHA was confirmed by the absorption bands observed at 1470–1420 and 875 cm^{-1}. Absorption band of PO_4^{3-}/HPO_4^{2-} belonged to CDHA at 1040–1020 cm^{-1} was also observed on FTIR data of PLA/CDHA fibers, which confirmed the presence of CDHA nanocrystals in PLA/CDHA fibers. PLA/CDHA fibers also showed a new absorption peak appeared at 1600 cm^{-1} as compared to PLA and CDHA nanocrystals.

Images of Fig. 3a through Fig. 3g were the results of SEM characterization. As shown in Fig. 3a, CDHA precipitates were consisted of needle-like nano-crystals. In Fig. 3b, the presence of elements Mg and Na in precipitates were observed by EDX analysis. XRD and FTIR data demonstrated above combined with the EDX analysis proved the precipitates were exactly CDHA. PLA fibers electrospun with different organic solvents composition are shown in Fig. 3c and d, higher DMF ratio in solvent not only reduced fibers diameter but also eliminated porous surface of PLA fibers. Such differences were also observed in Fig. 3e and f, which were fibers from PLA/CDHA solution with different organic solvents ratios. The SEM images show that the size of the fibers was decreased by the incorporation of CDHA filler to PLA matrix (Fig. 3c and e, d and f). PLA/CDHA fibers shown in Fig. 3f are fibers in nano-size. The EDX elements mapping shown in Fig. 3g and h demonstrated the uniform distribution of precipitates in fibers.

TEM images of CDHA precipitates are shown in Fig. 4a. Precipitates were needle like nano-crystals with dimensions of 20–40 nm in *c*-axis. In Fig. 4b is the TEM images of PLA/CDHA fibers, where CDHA particles were dispersed in the internal channel of PLA matrix as fillers. Some CDHA agglomerates were also observed.

3.2 In vitro degradation tests

The comparison of degradation rate between CDHA and HA is shown in Fig. 5a. CDHA is also slightly more basic to cause pH of the solution to slightly increase as shown in Fig. 5b. Figure 5c is the mass loss behavior of PLA/CDHA fibers and PLA fibers in PBS, PLA/CDHA fibers showed a faster degradation rate as compared to PLA fibers. Fig. 5d is the pH change of PBS caused by degradation of PLA/CDHA and PLA fibers. Both fibers led to pH decrease in the first weeks, but the pH of PBS incubated with PLA/CDHA fibers was buffered back to almost 7.4 in the following weeks as compared to decreasing pH of PBS incubated with PLA fibers.

3.3 Bioactivity test

Results of bioactivity test were shown in Fig. 6. Both PLA and PLA/CDHA fibers surfaces were deposited with apatite (Fig. 6a, b). However, the apatite coating on PLA/CDHA fibers were more uniform. The XRD results also indicated the same results with stronger apatite peaks on PLA/CDHA fibers (Fig. 7).

3.4 Osteoblast cell culture

Results of in vitro cell culture are shown in Fig. 8. The results were compared by one-way ANOVA analysis: PLA/CDHA

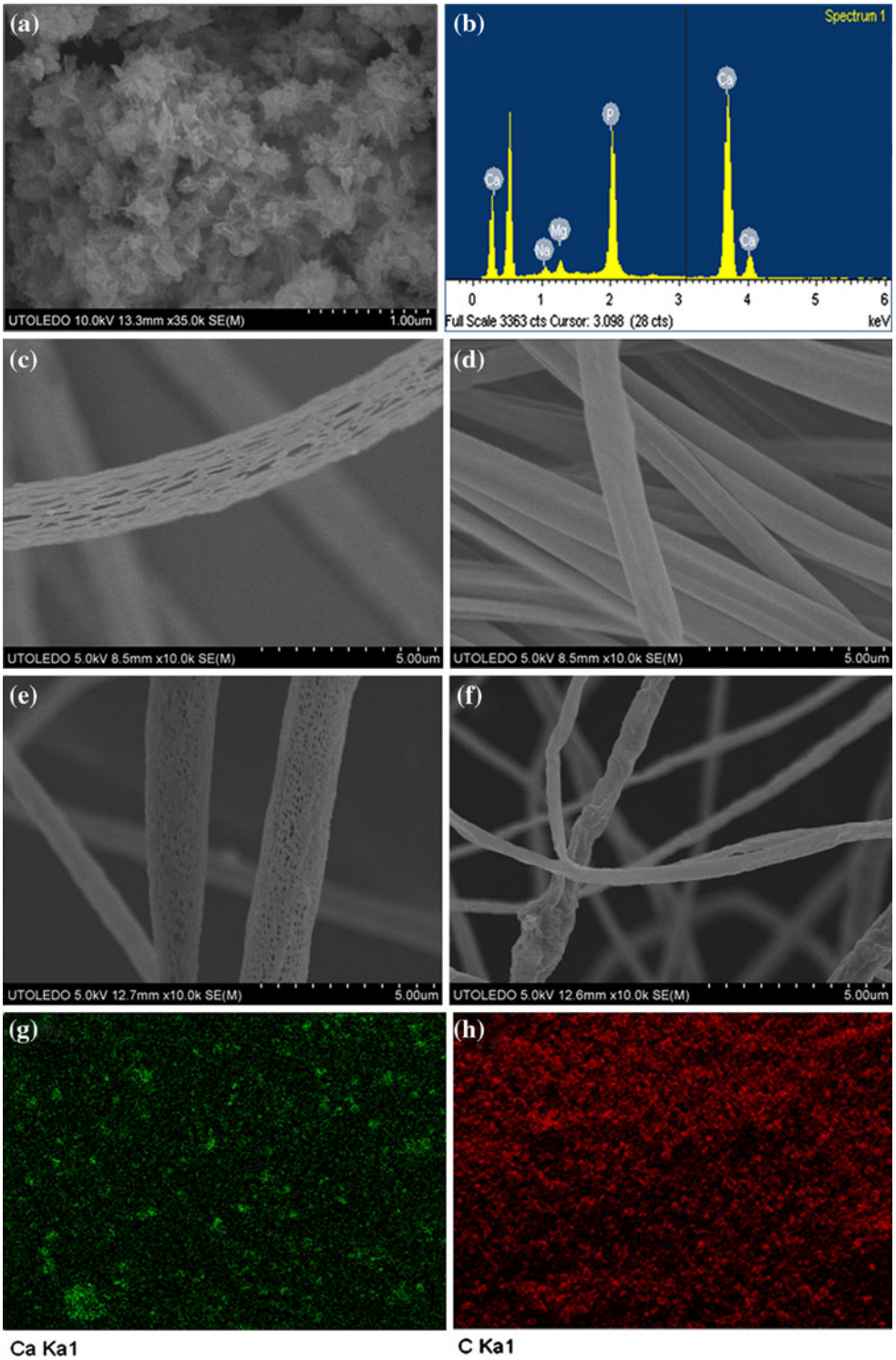

Fig. 3 Results of SEM characterization: **a** CDHA precipitates, **b** EDX analysis of CDHA precipitates, **c** PLA fibers, chloroform:DMF ratio is 9:1, **d** PLA fibers, chloroform:DMF ratio is 7:3, **e** PLA/CDHA fibers, chloroform:DMF ratio is 9:1, **f** PLA fibers, chloroform:DMF ratio is 7:3, **g** EDX mapping of Ca element, **h** EDX mapping of C element

electrospun fibers can promote osteoblast cells growth after 7 days as compared to PLA electrospun fibers and blank ($P < 0.05$). Osteoblast cells exhibited a flat appearance and were spread out over the surfaces of all samples. Formation of nano-CaP particles expressed by osteoblasts on PLA/CDHA fibers after 7 days was observed as shown in Fig. 9.

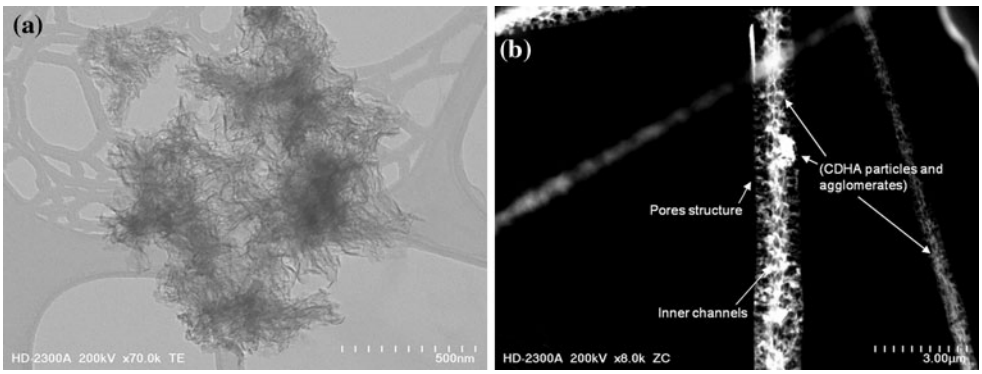

Fig. 4 TEM images of **a** CDHA precipitates, **b** PLA/CDHA fibers, chloroform:DMF ratio is 9:1

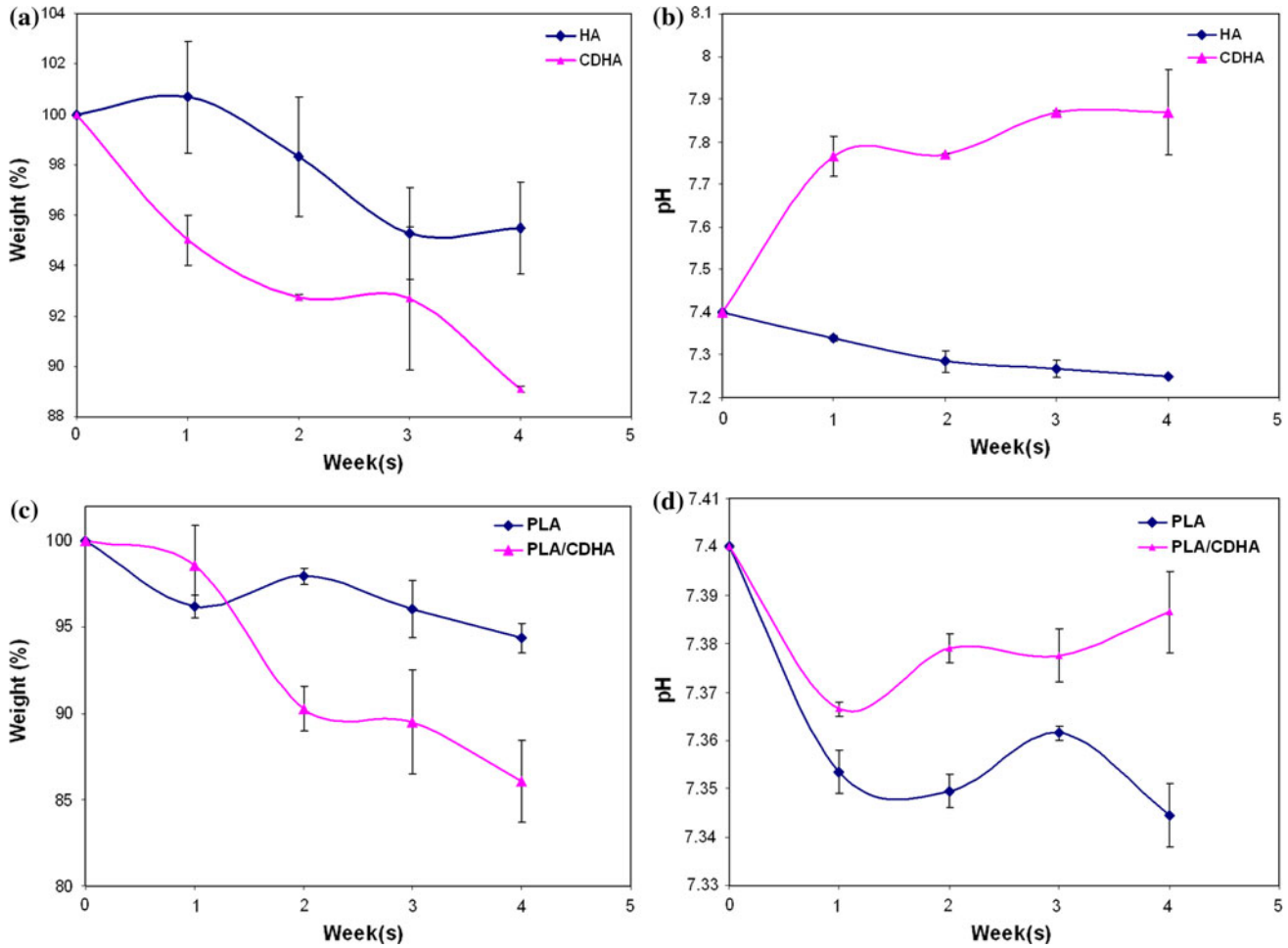

Fig. 5 Results of in vitro degradation test: **a** weight loss of CDHA and HA particles in PBS, **b** pH change of PBS caused by CDHA and HA degradation, **c** weight loss of PLA/CDHA and PLA fibers in PBS, **d** pH change of PBS caused by PLA/CDHA and PLA fibers degradation

4 Discussion

Bone-like CDHA is an important compound among CaP materials because of its bioactivity [28]. CDHA composition is relatively close to the mineral component of bone, which is poorly crystalline hydroxyapatite (HA) with small amounts of elements such as sodium (Na^+), potassium (K^+), magnesium (Mg^{2+}), and carbonate (CO_3^{2-}) present in the lattice structure, as compared to crystallized CaP materials. These extra elements were reported to influence cell attachment, proliferation of osteoblasts and help in bone metabolism [29, 30]. Based on the results of XRD, SEM, TEM, FTIR and EDX characterization of precipitates, bone-like CDHA nanocrystals were successfully

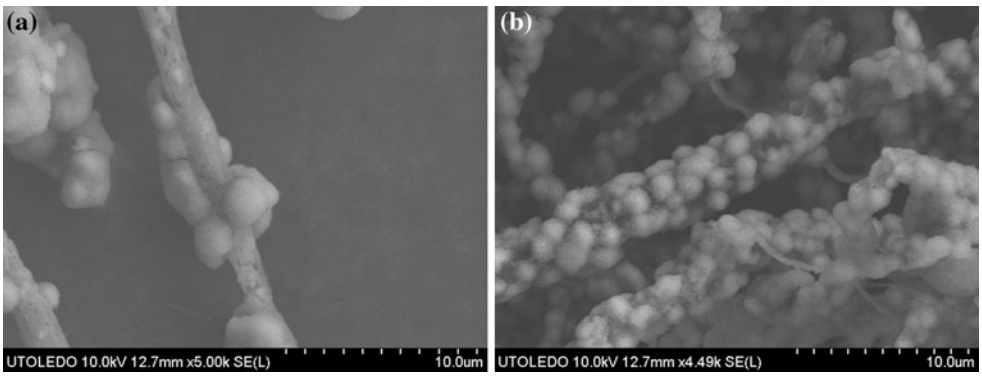

Fig. 6 SEM images of **a** PLA fibers after 1 week soaking in 1.5 × t-SBF, and **b** PLA/CDHA fibers after 1 week soaking in 1.5 × t-SBF

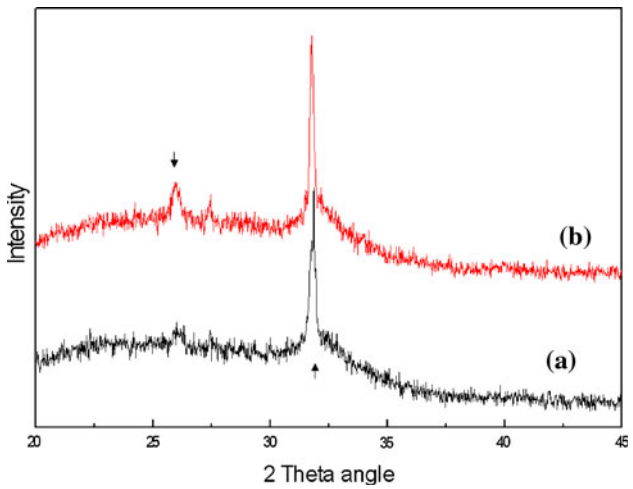

Fig. 7 XRD patterns of **a** PLA fibers after 1 week soaking in 1.5 × t-SBF, and **b** PLA/CDHA fibers after 1 week soaking in 1.5 × t-SBF

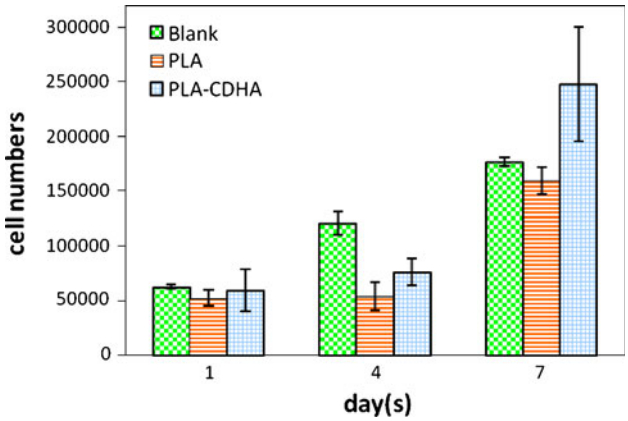

Fig. 8 Results of in vitro cell culture on blank, PLA and PLA/CDHA fibers

synthesized from the spontaneous precipitation occurred in modified 1.5 × t-SBF. The crystal domain size of CDHA precipitates was similar to that recorded deproteinated bone apatite, quantitatively confirmed by the similarity of the

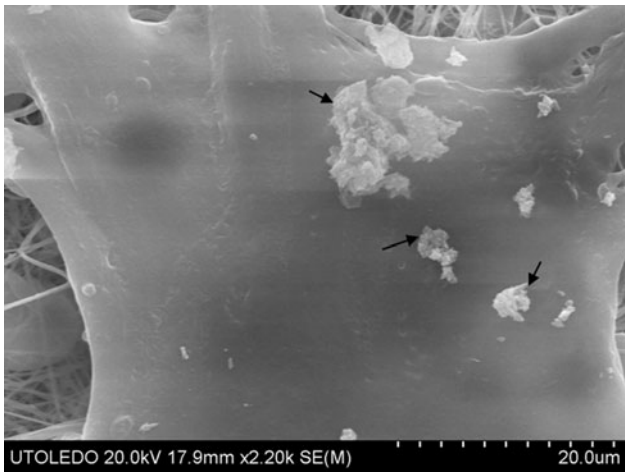

Fig. 9 SEM image of nano-CaP particles expressed by osteoblast cells after 7 days proliferation on PLA/CDHA fibers

two crystal domain sizes (210 and 213 Å, respectively) [31].

One function of addition of tris-base buffer in SBF is to make pH of SBF solution stable in a long period of time as described above. The purpose of reducing the tris-base amount is to intensify the precipitation of CDHA, and the result after 24 h precipitation fit the expectation. How to harvest CDHA precipitates is still a concern of CDHA application in industry in future. One possible approach is to use highly supersaturated SBF solution to produce precipitates with similar compositions as bone minerals [32, 33].

In degradation test, CDHA was observed to show a faster degradation as compared to stoichiometric HA, which can be attributed to the presence of trace elements in lattice structure. A pH increase caused by CDHA degradation in PBS was also observed. This behavior can be possibly attributed to a series of chemical reactions occurred in 1.5 × t-SBF during CDHA precipitation. A phenomenon that pH of SBF solution increased spontaneously and finally reached a stable value caused by

decomposition of bicarbonate ions has been reported before [34, 35]. In the CDHA precipitation process, OH^- ions are incorporated into the lattice structure of CDHA, which can be released into PBS to increase pH when degradation of CDHA occurred. Therefore, when CDHA nanocrystals were used as second phase in PLA matrix, they can buffer the pH decrease caused by the degradation of PLA as shown in Fig. 5d.

The incorporation of CaP materials with PLA has been a popular topic in biomaterial research. Many approaches were studied such as electrospinning, casting, and supercritical gas foaming [36]. However, no studies were reported on electrospun of CDHA and PLA bionanocomposite. This is the main highlight of this study. Electrospinning is a process to fabricate fibrous scaffold with high surface area and interconnected channels suitable for tissue regeneration. This process can be operated at ambient temperature, which is beneficial to the preservation of carbonate in CDHA lattice. Additionally, such electrospun PLA/CDHA scaffold shows possibility to be used as biomolecules delivery system. PLA is a conventional biodegradable material used for drug carrier, and act as barrier to avoid robust release of carried molecules; CDHA can work as drug loading sites for bio-molecules.

The XRD patterns and FTIR data of PLA/CDHA fibers (Fig. 1, 2) confirmed the presence of CDHA and PLA in the composite fibers. The results were similar to PLA/HA fibers reported in the literature before [37]. The new absorption band of PLA/CDHA fibers observed on FTIR was assigned to COO^- resulting from the interaction of COOH in PLA with Ca^{2+} in CDHA lattice. Therefore, CDHA precipitates were not only dispersed in the PLA matrix, but also reacted with PLA, resulting in chemical bonding between each other.

As shown in Fig. 3, the compositions of solvents were observed to influence fibers morphology. Higher DMF content not only decreased fibers diameter but also eliminated porous structure on fiber surface. Its effect on fiber diameter is attributed to its higher conductivity as compared to chloroform, which consequently increased electromagnetic force during electrospinning which stretched jet into thinner fibers [7]. The difference in pore structure can be explained by the volatility difference between DMF and chloroform. The low volatility of DMF led to a decrease in the evaporation rate of the mixed solvents to form stable jet being injected from the needle during electrospinning. Otherwise, quick evaporation caused by chloroform produced pores on PLA fibers surface. Such phenomenon caused by quick solvent evaporation was also described previously in electrospinning of biopolymers [38, 39]. The incorporation of CDHA to PLA matrix can also decrease fibers diameter, which is related to the change in viscosity of PLA solution caused by CDHA additives and the chemical bonding formed between CDHA and PLA in PLA/CDHA fibers. Due to dual effects of DMF and interaction between PLA/CDHA, fibers diameter was further reduced.

The TEM images of electrospun PLA/CDHA fibers showed dispersion of CDHA in PLA matrix (Fig. 4b). Only PLA/CDHA fibers (chloroform:DMF ratio is 9:1) were characterized using TEM because small diameter fibers get easily damaged by electron beam in TEM. The use of zeta contrast mode provided some benefits for fibers characterization as compared to normal TEM. First, the intra-fiber structure formed on the fibers surface was analyzed. Internal channels were observed with connections to outer pores. Therefore, PLA works as a shield with other co-electrospun materials in the inner cores, and such nanopores can potential provide channels for bio-molecules diffusion. Second, the existence of CDHA and its dispersion level can also be characterized. As shown in Fig. 4b, there are some agglomerates of CDHA particles in PLA/CDHA electrospun fibers. As described above, CDHA particles were formed via nucleation during precipitation process, which usually promotes some weak bonding between the CDHA nanocrystals. Therefore, physical force applied via ultrasonication in this experiment was not strong enough to destroy such bonding; stronger ultrasonication or external physical force is necessary in future to finely disperse CDHA particles.

The in vitro degradation test showed incorporation of CDHA to PLA matrix promotes faster degradation rate. This mechanism of degradation of PLA matrix with added CDHA is similar to degradation of PLGA with added TCP (tricalcium phosphate.) In an experiment reported by Loher et al. [40], pure PLGA matrix only had 0.5% mass loss and 2% water uptake after 6 weeks, while 30% α-TCP incorporation resulted in 7% mass loss and 14% water uptake after 6 weeks. The high degradation rate of α-TCP particles generated pores in the composite to result in a larger polymer surface being exposed to the surrounding media to promote PLGA degradation. It is believed that the same mechanism is applicable in this case as well. A larger section of PLA surface is exposed to the surrounding media due to the degradation of CDHA. The accumulation of hydrophilic degradation products of CDHA inside the PLA/CDHA fibers, further draws media into PLA matrix during the whole degradation process. In comparison, in previously published papers about PLA/HA electrospun fibers, HA acted as a physical barrier and blocked off the entry of water to slow down PLA degradation [38, 41]. The most important result of pH monitoring is that the adverse effects caused by PLA degradation can be overcome by the buffering effect of CDHA.

Formation of apatite on the surface of samples depends on the materials' intrinsic ability to form apatite in SBF.

The ability of biomaterials to develop bone-like apatite upon soaking in SBF has been correlated to bone bonding formation ability in vivo [42]. Both CDHA nanocrystals and PLA can play roles in apatite deposition. CDHA nanocrystals were similar to apatite formed in 1.5 × t-SBF, which can work as nucleation sites for apatite deposition. The apatite formation mechanism PLA is related to the hydrolysis of PLA, which results in a negatively charged PLA surface. The positively charged calcium ions in the solution are attracted to the hydrolyzed PLA surface and apatite forms through the attraction of phosphate groups from the solution [26]. The difference of coating thickness and uniformity observed between PLA and PLA/CDHA fibers can be attributed the incorporation of CDHA into the PLA matrix to intensify the apatite coating formation. Therefore, the apatite formation on PLA/CDHA coatings demonstrates their potential bone bonding ability.

Incorporation of CDHA into PLA matrix promotes osteoblasts cells proliferation as shown in Fig. 8, which further corroborates the results of bioactivity test. The results confirmed the important role of the CDHA in the stimulation of osteoblast cell response and thus its significance in the bone regeneration.

Based on these results, PLA/CDHA electrospun fibers can be applied for potential bone tissue regeneration. More studies are still required to assess the practical usefulness of this composite fiber, such as the assessment of bone tissue engineering potential with stem cells.

5 Conclusions

In this study, bone-like carbonated calcium deficient nanocrystalline CDHA particles were synthesized using a biomimetic technique using 1.5 × t-SBF. Ultrasonication of CDHA nanocrystals and choice of chloroform and DMF in certain ratios (7:3) led to the uniform distribution of CDHA in PLA resulting in bionanocomposites with each of the constituents with one dimension in nanometer scale. The results show that the incorporation of CDHA decreased PLA fiber diameters, accelerated PLA degradation, buffered pH decrease caused by PLA degradation, improved the bioactivity and biocompatibility of the scaffold. Such PLA/CDHA bionanocomposite has the potential to be used in tissue regeneration applications.

Acknowledgments This work was supported by a NSF Grant.

References

1. Sill TJ, von Recum HA. Electrospinning: applications in drug delivery and tissue engineering. Biomaterials. 2008;29:1989–2006.
2. Roy RA, Roy R. Diphasic xerogels: I ceramic-metal composites. Mater Res Bull. 1984;19:169–77.
3. Roy R, Komarneni S, Roy DM. Better ceramics through chemistry. Mater Res Soc Symp Proc. 1984;32:347–59.
4. Komarneni S. Nanocomposites. J Mater Chem. 1992;2:1219–30.
5. Darder M, Aranda P, Ruiz-Hitzky E. Bionanocomposites: a new concept of ecological, bioinspired, and functional hybrid materials. Adv Mater. 2007;19:1309–19.
6. Middleton JC, Tipton AJ. Synthetic biodegradable polymers as orthopedic devices. Biomaterials. 2000;21:2335–46.
7. Lassalle V, Ferreira ML. PLA nano- and microparticles for drug delivery: an overview of the methods of preparation. Macromol Biosci. 2007;7:767–83.
8. Yamaguchi M, Shinbo T, Kanamori T, Wang PC, Niwa M, Kawakami H, Nagaoka S, Hirakawa K, Kamiya M. Surface modification of poly(L-lactic acid) affects initial cell attachment, cell morphology, and cell growth. J Artif Organs. 2004;7:187–93.
9. Bergsma JE, Rozema FR, Bos RRM, Boering G, de Bruijn WC. Late degradation tissue response to poly(L-lactide) bone plates and screws. Biomaterials. 1995;16:25–31.
10. Jeong SI, Ko EK, Yum J, Jung CH, Lee YM, Shin H. Nanofibrous poly(lactic acid)/hydroxyapatite composite scaffolds for guided tissue regeneration. Macromol Biosci. 2008;8:328–38.
11. McCullen SD, Zhu Y, Bernacki SH, Narayan RJ, Pourdeyhimi B, Gorga RE, Loboa EG. Electrospun composite poly(L-lactic acid)/tricalium phosphate scaffolds induce proliferation and osteogenic differentiation of human adipose-derived stem cells. Biomed Mater. 2009;4:035002.
12. Roeder RK, Converse GL, Kane RJ, Yue W. Hydroxyapatite-reinforced polymer biocomposites for synthetic bone substitutes. JOM. 2008;60:38–45.
13. Rey C. Calcium phosphate biomaterials and bone mineral. Differences in composition, structure and properties. Biomaterials. 1990;11:13–5.
14. Wang X, Song G, Lou T. Fabrication and characterization of nano composite scaffold of poly(L-lactic acid)/hydroxyapatite. J Mater Sic: Mater Med. 2010;21:183–8.
15. Kokubo T. Surface chemistry of bioactive glass-ceramics. J Non-Cryst Solids. 1990;120:138–51.
16. Tas AC. Synthesis of biomimetic Ca-hydroxyapatite powders at 37°C in synthetic body fluids. Biomaterials. 2000;21:1429–38.
17. Bigi A, Boanini E, Panzavolta S, Roveri N. Biomimetic growth of hydroxyapatite on gelatin films doped with sodium polyacrylate. Biomacromolecules. 2000;1:752–6.
18. Dorozhkina EI, Dorozhkin SV. Surface mineralization of hydroxyapatite in modified simulated body fluid (mSBF) with higher amounts of hydrogencarbonate ions. Colloid Surface A. 2002;210:41–8.
19. Oyane A, Onuma K, Ito A, Kim HM, Kokubo T, Nakamura T. Formation and growth of clusters in conventional and new kinds of simulated body fluids. J Biomed Mater Res. 2003;64:339–48.
20. Jalota S, Bhaduri SB, Tas AC. Effect of carbonate content and buffer type on calcium phosphonate formation in SBF solutions. J Mater Sci Mater Med. 2006;17:697–707.
21. Jalota S, Bhaduri SB, Tas AC. Using a synthetic body-fluid (SBF) solution of 27 mM HCO_3^- to make bone substitutes more osteointegrative. Mater Sci Eng C. 2008;28:129–40.
22. Yin X, Stoot MJ. Biological calcium phosphates and posner's cluster. J Chem Phys. 2003;118:3717–23.
23. Onuma K, Ito A. Cluster growth model for hydroxyapatite. Chem Mater. 1998;10:3346–51.
24. Qu H, Wei M. The effect of temperature and initial pH on biomimetic apatite coating. J Biomed Mater Res B Appl Biomater. 2008;87:204–12.

25. Durucan C, Brown PW. Low temperature formation of calcium-deficient hydroxyapatite-PLA/PLGA composites. J Biomed Med Res. 2000;51:717–25.
26. Zhang R, Ma PX. Porous poly(L-lactic acid)/apatite composites created by biomimetic process. J Biomed Mater Res. 1999;45: 285–93.
27. Rakovsky A, Gutmanas EY, Gotman I. Ca-deficient hydroxyapatite/polylactide nanocomposites with chemically modified interfaces by high pressure consolidation at room temperature. J Mater Sci. 2010;45:6339–44.
28. Dorozhkin SV, Epple M. Biological and medical significance of calcium phosphates. Angew Chem Int Ed. 2002;41:3130–46.
29. Tylavsky FA, Spence LA, Harkness L. The importance of calcium, potassium, and acid-base homeostasis in bone health and osteoporosis prevention. J Nutri. 2008;138:164S–5S.
30. Takeda R, Nakamura T. Effects of high magnesium intake on bone mineral status and lipid metabolism in rats. J Nutri Sci Vitam. 2008;54:66–75.
31. Palazzo B, Iafisco M, Laforgia M, Margiotta N, Natile G, Bianchi CL, Walsh D. Mann Stephen, Roveri Norberto. Biomimetic hydroxyapatite-drug nanocrystals as potential bone substitutes with antitumor drug delivery properties. Adv Funct Mater. 2007;17:2180–8.
32. Tas AC, Bhaduri SB. Rapid coating of Ti6Al4 V at room temperature with a calcium phosphate solution similar to 10× simulated body fluid. J Mater Res. 2004;19:2742–9.
33. Hofmann I, Müller L, Greil P, Müller FA. Precipitation of carbonated calcium phosphate powders from a highly supersaturated simulated body fluid solution. J Am Ceram Soc. 2007;90:821–4.
34. Oyane A, Kim HM, Furuya T, Kokubo T, Miyazaki T, Nakamura T. Preparation and assessment of revised simulated body fluids. J Biomed Mater Res. 2003;65:188–95.
35. Wen HB, de Wijn JR, Cui FZ, de Groot K. Preparation of calcium phosphonate coatings on titanium implant materials by simple chemistry. J Biomed Mater Res. 1998;41:227–36.
36. Dorozhkin SV. Calcium orthophosphate-based biocomposites and hybrid biomaterials. J Mater Sci. 2009;44:2343–87.
37. Sui G, Yang X, Mei F, Hu X, Chen G, Deng X, Ryu S. Poly-L-lactic acid/hydroxyapatite hybrid membrane for bone tissue regeneration. J Biomed Mater Res A. 2007;82:445–54.
38. Megelski S, Stephens JS, Chase DB, Rabolt JF. Micro- and nanostructured surface morphology on electrospun polymer fibers. Macromolecules. 2002;35:8456–66.
39. Bognitzki M, Czado W, Frese T, Schaper A, Hellwing M, Steinhart M, Greiner A, Wenorff JH. Nanostructured fibers via electrospinning. Adv Mater. 2001;13:70–2.
40. Loher S, Reboul V, Brunner TJ, Simonet M, Dora C, Neuenschwander P, Stark WJ. Improved degradation and bioactivity of amorphous aerosol derived tricalcium phosphate nanoparticles in poly(lactide-co-glycolide). Nanotech. 2006;17:2054–61.
41. Deng XL, Sui G, Zhao ML, Chen GQ, Yang XP. Poly(L-lactic acid)/hydroxyapatite hybrid nanofibrous scaffolds prepared by electrospinning. J Biomed Sci Polymer Edn. 2007;18:117–30.
42. Kokubo T, Takadama H. How useful is SBF in predicting in vivo bone bioactivity? Biomaterials. 2006;27:2907–15.